ChemComm

COMMUNICATION

View Article Online
View Journal | View Issue

Cite this: *Chem. Commun.*, 2026, **62**, 6114

Received 26th January 2026,
Accepted 25th February 2026

DOI: 10.1039/d6cc00518g

rsc.li/chemcomm

Mechanochemical applications of magnesium nitride to fullerene chemistry: synthesis of pyrroline-fused tetra-functionalized [60]fullerene derivatives

Jun-Shen Chen,[a] Wen-Jie Qiu,[a] Li-Feng Guo[a] and Guan-Wu Wang *[abc]

A novel application of magnesium nitride (Mg_3N_2) for the synthesis of pyrroline-fused tetra-functionalized [60]fullerene (C_{60}) derivatives is reported under solvent-free ball-milling conditions. This approach represents the first mechanochemical method to regioselectively achieve tetra-functionalization of C_{60}. Notably, the present protocol enables efficient incorporation of nitrogen from Mg_3N_2 directly into fullerene products.

Mechanochemical organic transformations have become increasingly important over the past three decades.[1] One of the charms of mechanochemistry is the ability to synthesize and functionalize compounds such as fullerenes that are insoluble or poorly soluble in common solvents. It is well known that fullerene derivatives have great potential applications in materials, biology and nanoscience.[2] However, the functionalization of fullerenes is severely limited due to their poor solubility in common organic solvents. Thus, the emergence of mechanochemistry opens up more possibilities for constructing fullerene derivatives.[3] The application of mechanochemistry to fullerene chemistry was first reported in 1996.[4] To date, various syntheses of di- and multi-functionalized fullerenes have been reported, but methods for synthesizing multi-functionalized fullerenes in solutions often yield multiple regioisomers.[3a,5] Therefore, it is of great significance to develop methods for the synthesis of single isomers of multi-adducts of [60]fullerene (C_{60}) under solvent-free conditions.

Some inorganic salts, such as calcium carbide, have been used in organic synthesis as solid alternatives to gaseous reagents, despite their insolubility in organic solvents.[6] Magnesium nitride (Mg_3N_2), a commercially available and stable solid, has significant potential to replace ammonia in organic synthesis by serving as a solid surrogate. However, up to now, there are only a few reports on both solution-based and solvent-free applications of Mg_3N_2.[7] Furthermore, reactions performed in solution phases required high temperatures and long reaction times owing to poor solubility (Scheme 1a).[7a–d] Nevertheless, Mg_3N_2 conversion does not always require a solvent and may even be accelerated under solvent-free conditions. In 2021, González and Menéndez reported the first mechanochemical synthesis of primary amides, but still used a large quantity of ethanol as a proton source (Scheme 1b).[7e]

Motivated by the potential of fullerene mechanochemistry, we aim to bypass the poor solubility of both fullerenes and

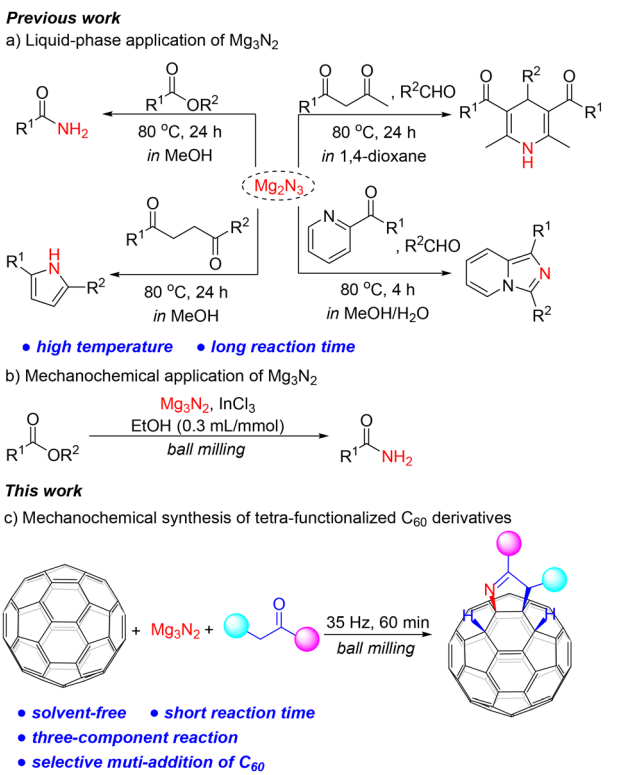

Scheme 1 (a) Liquid-phase and (b, c) mechanochemical applications of Mg_3N_2 for the synthesis of *N*-containing compounds.

[a] *Department of Chemistry, University of Science and Technology of China, Hefei, Anhui 230026, P. R. China. E-mail: gwang@ustc.edu.cn*
[b] *Key Laboratory of Functional Molecular Solids, Ministry of Education, Anhui Laboratory of Molecule-Based Materials, and School of Chemistry and Materials Science, Anhui Normal University, Wuhu, Anhui 241002, P. R. China*
[c] *State Key Laboratory of Natural Product Chemistry, Lanzhou University, Lanzhou, Gansu 730000, P. R. China*

Mg_3N_2 by employing mechanical milling to synthesize C_{60} derivatives quickly and efficiently. Herein, we report the mechanosynthesis of tetra-functionalized C_{60} derivatives featuring a pyrroline heterocycle fused to a [6,6]-bond *via* one-pot three-component reaction. Notably, this is also the first regioselective synthesis of multi-functionalized derivatives of C_{60} under solvent-free conditions.

We began optimizing the conditions for the mechanochemical reaction of C_{60} with Mg_3N_2 and acetophenone. Initially, a mixture of C_{60} (0.04 mmol), 5.0 equiv. of Mg_3N_2 and 10.0 equiv. of acetophenone was milled in the presence of 1.0 equiv. of silver chloride (AgCl) and 36.0 mg of silica gel (200–300 mesh) as grinding auxiliary[8,9] at a frequency of 35 Hz at room temperature for 1 h. Pleasingly, a tetra-functionalized product **2a** was obtained regioselectively in 27% yield (Table 1, entry 1). Increasing the amount of acetophenone to 15.0 equiv. significantly improved the yield to 37%. However, further increasing the quantity of acetophenone to 20.0 equiv. gave a slightly lower yield (Table 1, entries 2 and 3). In addition, neither increasing nor decreasing the amount of Mg_3N_2 had any benefit to yields (Table 1, entries 4 and 5). We also investigated the amount of AgCl. When the reaction was performed without AgCl, the product yield was reduced to 14% (Table 1, entry 6). What's more, reactions with 0.5 and 1.5 equiv. of AgCl gave lower yields of 26% and 29%, respectively (Table 1, entries 7 and 8). Based on the above results, it is clear that the AgCl is not a determining factor. To exclude the effect of the chloride ion in AgCl, sodium chloride (NaCl) was used to replace AgCl, but it did not promote the reaction (Table 1, entry 9). Next, it was found that the use of zinc chloride ($ZnCl_2$) and magnesium chloride ($MgCl_2$) as Lewis acids provided a modest enhancement of the reaction compared to the non-additive conditions (Table 1, entries 10 and 11 *vs.* entry 6). Therefore, AgCl was considered to be a very weak Lewis acid interacting with the carbonyl group in the substrate. Some commonly used silver salts were also screened to improve the yield. Among them, silver bromide (AgBr) and silver nitrate ($AgNO_3$) achieved yields of 22% and 23%, respectively (Table 1, entries 12 and 13). However, silver carbonate (Ag_2CO_3) and silver acetate (AgOAc), which possess weakly basic counteranions, only gave a trace yield and a 9% yield, respectively (Table 1, entries 14 and 15). Furthermore, without the use of silica gel as a grinding auxiliary, only a small amount of **2a** could be obtained (Table 1, entry 16). In addition, we also tried to decrease the milling frequency to obtain a higher yield. However, this resulted in a slight reduction in yield (Table 1, entry 17). Replacing Mg_3N_2 with the more reactive calcium nitride (Ca_3N_2) led to the complete consumption of C_{60} but yielded no product (Table 1, entry 18).

Table 1 Optimization of the reaction conditions[a]

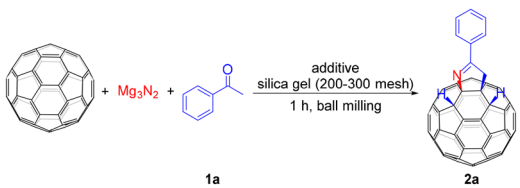

Entry	Molar ratio of C_{60}/Mg_3N_2/**1a**	Additive (equiv.)	Yield of **2a**[b] (%)
1	1 : 5 : 10	AgCl (1.0)	27 (36)
2	**1 : 5 : 15**	**AgCl (1.0)**	**37 (51)**
3	1 : 5 : 20	AgCl (1.0)	31 (46)
4	1 : 3 : 15	AgCl (1.0)	28 (39)
5	1 : 7 : 15	AgCl (1.0)	32 (39)
6	1 : 5 : 15	0	14 (15)
7	1 : 5 : 15	AgCl (0.5)	26 (30)
8	1 : 5 : 15	AgCl (1.5)	29 (37)
9	1 : 5 : 15	NaCl (1.0)	12 (13)
10	1 : 5 : 15	$ZnCl_2$ (1.0)	17 (71)
11	1 : 5 : 15	$MgCl_2$ (1.0)	23 (74)
12	1 : 5 : 15	AgBr (1.0)	22 (25)
13	1 : 5 : 15	$AgNO_3$ (1.0)	23 (36)
14	1 : 5 : 15	Ag_2CO_3 (0.5)	Trace
15	1 : 5 : 15	AgOAc (1.0)	9 (9)
16[c]	1 : 5 : 15	AgCl (1.0)	Trace
17[d]	1 : 5 : 15	AgCl (1.0)	29 (39)
18[e]	1 : 5 : 15	AgCl (1.0)	0

[a] Unless otherwise noted, all reactions were performed with C_{60} (0.04 mmol), Mg_3N_2, **1a**, additive and silica gel (36.0 mg, 200–300 mesh) together with four stainless balls (5 mm in diameter) in a stainless jar (5 mL) and were milled vigorously (35 Hz) at room temperature for 1 h. [b] Isolated yields were based on C_{60}. Values in parentheses were based on consumed C_{60}. [c] No silica gel. [d] The milling frequency was 30 Hz. [e] Ca_3N_2 was used instead of Mg_3N_2.

Having optimized the reaction under solvent-free conditions, we then investigated its performance in different volumes of toluene (Fig. 1). As illustrated in Fig. 1, the liquid-phase reaction in toluene for 1 h at room temperature gave the product **2a** in only 3–6% yields. These results demonstrate the unique advantages of mechanochemical methods in the synthesis of fullerene derivatives. By eliminating solvents, mechanochemistry not only enables higher reactant concentrations but also overcomes the challenge of poor solubility of fullerenes, thereby significantly enhancing the reaction efficiency.

With the optimized reaction conditions in hand, a series of ketones were evaluated to investigate the substrate scope of this three-component reaction (Scheme 2). Firstly, acetophenones (**1b** and **1c**) with electron-withdrawing substituents (Cl and Br) at the *para*-position were well tolerated in this transformation and afforded desired products **2b** and **2c** in yields of 36% and 29%, respectively. It is worth mentioning that the dosage was

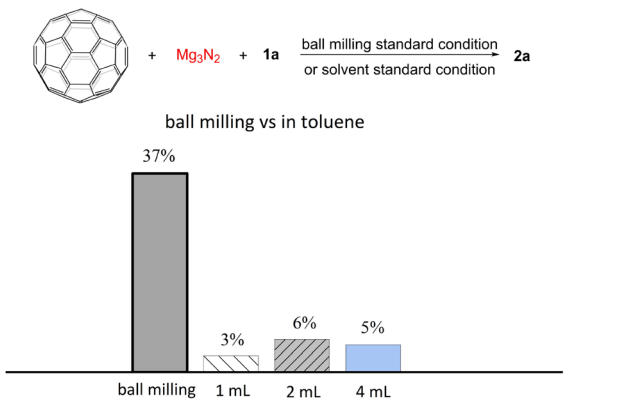

Fig. 1 Comparison with liquid-phase system. Solvent conditions: C_{60} (0.04 mmol), Mg_3N_2 (0.20 mmol), acetophenone (0.60 mmol), AgCl (0.04 mmol), silica gel (36.0 mg, 200–300 mesh) and toluene (1, 2 or 4 mL), r.t., 1 h.

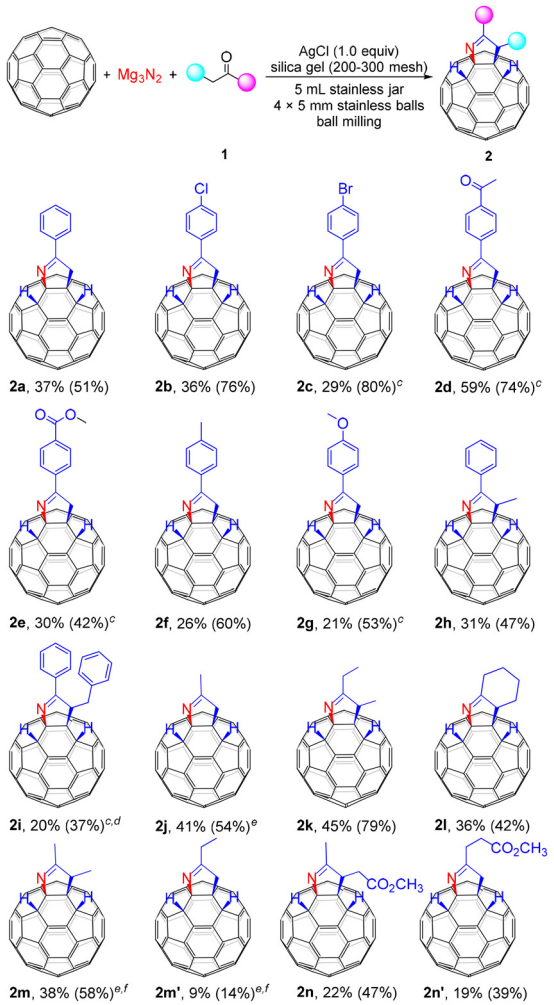

Scheme 2 Reactions of C_{60} with ketones and Mg_3N_2. [a] Unless otherwise specified, all reactions were performed with 0.04 mmol of C_{60}, Mg_3N_2 (0.20 mmol), **1** (0.60 mmol), AgCl (0.04 mmol) and silica gel (36.0 mg, 200–300 mesh) together with four stainless-steel balls (5 mm in diameter) in a stainless-steel jar (5 mL) and milled vigorously (35 Hz) at room temperature for 1 h. [b] Isolated yields were based on C_{60}. Values in parentheses were based on consumed C_{60}. [c] 0.40 mmol of **1** was used. [d] The reaction was performed at 40 Hz for 1.5 h. [e] 0.80 mmol of **1** was used. [f] 30 Hz was used.

reduced to 10.0 equiv. when using the solid **1c**. The same is true for other solid substrates. Satisfyingly, 1,4-diacetylbenzene (**1d**) possessing two acetyl groups afforded product **2d** in 59% yield. When methyl 4-acetylbenzoate (**1e**) was used, the ester group remained intact, affording the desired product **2e** in 30% yield. With the enhancement of the electron-donating effect, *p*-methyl- and *p*-methoxy-substituted acetophenones (**1f** and **1g**) provided **2f** and **2g** in yields of 26% and 21%, respectively. Propiophenone (**1h**) and β-phenyl propiophenone (**1i**) could also participate in this reaction and gave the desired products **2h** and **2i** in 31% and 20% yields, respectively. Next, we examined the compatibility of aliphatic ketones. It was found that aliphatic ketones were well suitable for this reaction. Considering that acetone (**1j**) is highly volatile, 20.0 equiv. of acetone were used and provided the desired product **2j** in 41% yield. 3-Pentanone (**1k**) and cyclohexanone (**1l**) were also amenable to this transformation, affording products **2k** and **2l** in 45% and 36% yields, respectively. When the unsymmetrical 2-butanone (**1m**) was tested, two isomers **2m** and **2m′** were isolated in 38% and 9% yields, respectively. Satisfactorily, the ester group in methyl acetylacetonate was tolerated and did not participate in the reaction, resulting in a pair of isomers **2n** and **2n′** with yields of 22% and 19%, respectively.

To determine the structures of products **2a**–**n′**, they were characterized by matrix-assisted laser desorption/ionization time-of-flight high-resolution mass spectrometry (MALDI-TOF HRMS), ^{1}H and ^{13}C nuclear magnetic resonance (NMR), Fourier-transform infrared spectroscopy (FTIR), ultraviolet–visible (UV–vis), cyclic voltammetry (CV) and differential pulse voltammetry (DPV) spectra (see SI). Their ^{1}H NMR spectra displayed the expected chemical shifts, and there was coupling between the two hydrogen atoms, with a coupling constant of 1.7–1.8 Hz, indicating that they were in the *para*-position on the six-membered ring. In the ^{13}C NMR spectra, there were at least 50 peaks for the 56 sp^2 carbons of the C_{60} cage and 4 peaks for the four sp^3 carbons of the C_{60} moiety. Furthermore, the structure of **2c** was unambiguously established by X-ray crystallography (Fig. 2).

To investigate the potential role of Mg_3N_2 as an ammonia surrogate, when it was directly replaced with aqueous ammonia ($NH_3{\cdot}H_2O$), the target product was obtained in only 3% yield. This result indicated that the direct condensation of ammonia, potentially generated from Mg_3N_2, with ketones was not the dominant pathway. Therefore, the nitride anion may directly condense with the used ketone or act as a base to remove the α-hydrogen of ketones or derivatives. Next, we further investigated the origin of the hydrogen atoms attached to the fullerene cage. Deuterated acetone (D, 99%) was selected as the starting material. The resulting product **2j-D** was analyzed by ^{1}H NMR spectroscopy. It was found that about equal amounts of deuterium atoms at the H_c and H_d positions underwent D/H exchange during the milling process, promoted by the strong base Mg_3N_2 (Fig. 3). In addition, the H/D ratio at H_b was comparable to that for each one at H_c and H_d positions, suggesting that an H/D scrambling equilibrium at these positions had been established during the reaction. This result indicates the presence of proton sources in the reaction system, likely originating from Si–OH groups of silica gel or residual water. Interestingly, the H/D ratio at H_a was found to be higher than that at H_b. The assignments of H_a and H_b were established based on the HMBC spectra of **2a** and **2j** (Fig. S54 and S83).

Based on the control experiments, a plausible reaction mechanism is proposed (Scheme 3). First, deprotonation at the α-carbon of ketone **1** by Mg_3N_2 generates carbanion $\mathbf{1}^-$, which undergoes nucleophilic addition to C_{60} to form fullerenyl anion **A**, with Mg^{2+} serving as the countercation. Protonation of the anionic

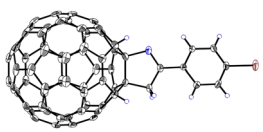

Fig. 2 Oak ridge thermal ellipsoid plot (ORTEP) diagrams for compound **2c** with 20% thermal ellipsoids. The solvent molecules are omitted for clarity.

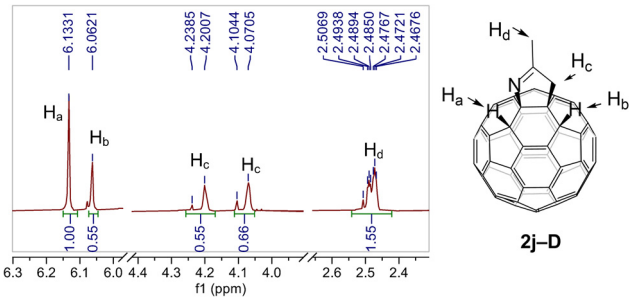

Fig. 3 ^{1}H NMR of **2j-D** obtained using acetone-D_6 (D, 99%).

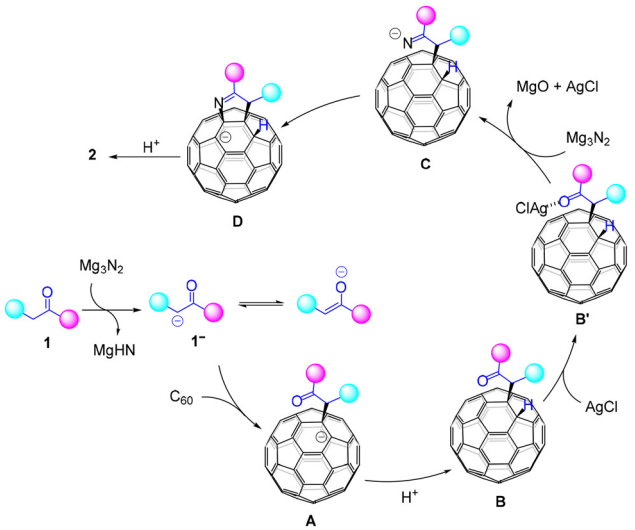

Scheme 3 Proposed reaction mechanism.

species **A** by the proton source present in the reaction system provides **B**. The nitride anion in Mg_3N_2 condenses with the carbonyl group in **B** with the assistance of AgCl, leading to the formation of the anionic ketoimine species **C** *via* the complex **B′**. This imine anion undergoes nucleophilic addition to the fullerene cage, providing an anionic intermediate **D**. The countercation in both **C** and **D** is likely to be a Mg^{2+} species. Finally, **D** is protonated by the proton source present in the reaction mixture and/or during workup process[10] to afford the target product **2**.

In summary, we have developed a new method for synthesizing pyrroline-fused tetra-functionalized C_{60} derivatives by employing Mg_3N_2 as a nitrogen source and base under mechanochemical conditions. This approach overcomes the poor solubility of both fullerenes and Mg_3N_2, enabling the efficient and regioselective synthesis of tetra-functionalized C_{60} derivatives in a short time of 1 h under ambient air and at room temperature. This mechanochemical strategy broadens the utility of Mg_3N_2 and expands the toolbox of incorporating nitrogen atoms into organic compounds.

We are grateful for financial support from the National Natural Science Foundation of China (22271271, 21372211).

Conflicts of interest

There are no conflicts to declare.

Data availability

The data supporting the finding of this study are available in this article and its supplementary information (SI). Supplementary information: detailed experimental procedures, characterisation data, NMR, UV-vis, CV and DPV spectra of compounds **2a–n′** and X-ray data of **2c**. See DOI: https://doi.org/10.1039/d6cc00518g.

CCDC 2525038 contains the supplementary crystallographic data for this paper.[11]

References

1 (*a*) T. Friščić, *Chem. Soc. Rev.*, 2012, **41**, 3493–3510; (*b*) G.-W. Wang, *Chem. Soc. Rev.*, 2013, **42**, 7668–7700; (*c*) J. G. Hernández and C. Bolm, *J. Org. Chem.*, 2017, **82**, 4007–4019; (*d*) C. Bolm and J. G. Hernández, *Angew. Chem., Int. Ed.*, 2019, **58**, 3285–3299; (*e*) H. Wang, P. Ying, J. Yu and W. Su, *Chin. J. Org. Chem.*, 2021, **41**, 1897–1924; (*f*) P. Ying, J. Yu and W. Su, *Adv. Synth. Catal.*, 2021, **363**, 1246–1271; (*g*) A. C. Jones, J. A. Leitch, S. E. Raby-Buck and D. L. Browne, *Nat. Synth.*, 2022, **1**, 763–775; (*h*) V. Martinez, T. Stolar, B. Karadeniz, I. Brekalo and K. Uzarevic, *Nat. Rev. Chem.*, 2023, **7**, 51–65; (*i*) R. Liu, X. He, T. Liu, X. Wang, Q. Wang, X. Chen and Z. Lian, *Chem. – Eur. J.*, 2024, **30**, e202401376.

2 (*a*) M. Chen, R. Guan and S. Yang, *Adv. Sci.*, 2019, **6**, 1800941; (*b*) K. Harano and E. Nakamura, *Acc. Chem. Res.*, 2019, **52**, 2090–2100; (*c*) T. Umeyama and H. Imahori, *Acc. Chem. Res.*, 2019, **52**, 2046–2055; (*d*) Z. Xing, S.-H. Li and S. Yang, *Small Struct.*, 2022, **3**, 2200012.

3 (*a*) S.-E. Zhu, F. Li and G.-W. Wang, *Chem. Soc. Rev.*, 2013, **42**, 7535–7570; (*b*) G.-W. Wang, *Chin. J. Chem.*, 2021, **39**, 1797–1803.

4 G.-W. Wang, Y. Murata, K. Komatsu and T. S. M. Wan, *Chem. Commun.*, 1996, 2059–2060.

5 (*a*) H. W. Liu, H. Xu, G. Shao and G.-W. Wang, *Org. Lett.*, 2019, **21**, 2625–2628; (*b*) G. Shao, C. Niu, H. W. Liu, H. Yang, J. S. Chen, Y. R. Yao, S. Yang and G.-W. Wang, *Org. Lett.*, 2023, **25**, 1229–1234; (*c*) H. Yang, S.-Q. Ye, G. Shao, J.-S. Chen and G.-W. Wang, *Synlett*, 2023, **34**, 2047–2051; (*d*) G. Shao, Y.-Y. Liu, C. Niu, Z.-C. Yin, S.-Q. Ye, Y.-R. Yao, M. Chen, J.-S. Chen, X.-L. Xia, S. Yang and G.-W. Wang, *Chem. Sci.*, 2024, **15**, 14899–14904.

6 K. S. Rodygin, M. S. Ledovskaya, V. V. Voronin, K. A. Lotsman and V. P. Ananikov, *Eur. J. Org. Chem.*, 2021, 43–52.

7 (*a*) G. E. Veitch, K. L. Bridgwood and S. V. Ley, *Org. Lett.*, 2008, **10**, 3623–3625; (*b*) K. L. Bridgwood, G. E. Veitch and S. V. Ley, *Org. Lett.*, 2008, **10**, 3627–3629; (*c*) G. E. Veitch, K. L. Bridgwood, K. Rands-Trevor and S. V. Ley, *Synlett*, 2008, 2597–2600; (*d*) S. Long, M. Panunzio, A. Petroli, W. Qin and Z. Xia, *Synthesis*, 2011, 1071–1078; (*e*) S. G. Patil, J. S. Jadhav and S. T. Sankpal, *RSC Adv.*, 2020, **10**, 11808–11815; (*f*) J. Gómez-Carpintero, J. D. Sánchez, J. F. González and J. C. Menéndez, *J. Org. Chem.*, 2021, **86**, 14232–14237.

8 (*a*) Z. Li, Z. Jiang and W. Su, *Green Chem.*, 2015, **17**, 2330–2334; (*b*) C. S. Yadav, R. Suhasini, V. Thiagarajan, D. Velmurugan and S. Kannadasan, *ChemistrySelect*, 2018, **3**, 12576–12581; (*c*) R. Aggarwal, M. Hooda, P. Kumar and G. Sumran, *Lett. Org. Chem.*, 2021, **18**, 532–537.

9 (*a*) R. Thorwirth, A. Stolle and B. Ondruschka, *Green Chem.*, 2010, **12**, 985–991; (*b*) H.-G. Li and G.-W. Wang, *J. Org. Chem.*, 2017, **82**, 6341–6348; (*c*) D. Kong, M. M. Amer and C. Bolm, *Green Chem.*, 2022, **24**, 3125–3129; (*d*) D. Kong and C. Bolm, *Green Chem.*, 2022, **24**, 6476–6480; (*e*) C. Grundke, J. Groß, N. Vierengel, J. Sirleaf, M. Schmitz, L. Krieger and T. Opatz, *Org. Biomol. Chem.*, 2023, **21**, 644–650; (*f*) C.-M. Chen, J.-X. Chen and C. T. To, *Green Chem.*, 2023, **25**, 2559–2562; (*g*) K. Xiang, P. Ying, T. Ying, W. Su and J. Yu, *Green Chem.*, 2023, **25**, 2853–2862; (*h*) S. Saha, A. A. Bhosle, A. Chatterjee and M. Banerjee, *J. Org. Chem.*, 2023, **88**, 10002–10013; (*i*) S. Saha, A. B. Pinheiro, A. Chatterjee, Z. T. Bhutia and M. Banerjee, *Green Chem.*, 2024, **26**, 5879–5889.

10 H.-S. Lin, Y. Matsuo, J.-J. Wang and G.-W. Wang, *Org. Chem. Front.*, 2017, **4**, 603–607.

11 CCDC 2525038: Experimental Crystal Structure Determination, 2026, DOI: 10.5517/ccdc.csd.cc2qrhvv.